Continuum Mech. Thermodyn. (2026) 38:27
https://doi.org/10.1007/s00161-026-01458-4

ORIGINAL ARTICLE

**Nihal Ege · Barış Erbaş · Julius Kaplunov**

# Dynamics of a FGM thin elastic coating subject to anti-plane shear

Received: 7 December 2025 / Accepted: 5 February 2026
© The Author(s) 2026

**Abstract** A multimode long-wave asymptotic procedure is developed in the framework of a two-dimensional time-harmonic scalar problem for the dynamic anti-plane shear of a functionally graded (FGM) coating. The resulting reduced 1D equation explicitly depends on the frequency parameter extending previous results for homogeneous coatings. The associated dispersion relations provide accurate approximations of the exact spectrum near the vicinities of all cut-off frequencies and offer detailed insight into the dynamic response of the coating. The formulation is valid for a distributed loading and accurately captures long-wave, high-frequency dynamics across multiple modes, while short-wavelength effects remain outside its scope.

**Keywords** Anti-plane · Asymptotic · Functionally graded · Coating · Long-wave · Multimode

## 1 Introduction

In this work, a coating is interpreted as an elastic layer with one face clamped and the other subjected to prescribed surface stresses, consistent with the definitions given by [1], see also [2]. In contrast, for plates the boundary conditions typically involve prescribed stresses. In particular, it is well known that coatings do not exhibit the fundamental low-frequency vibration modes characteristic of thin structures with traction-free faces, e.g., see [3] and also [4]. The presence of a clamped face suppresses low-frequency modes, allowing only high-frequency ones, with cut-offs corresponding to thickness resonances. Previous studies have developed long-wave approximations near such cut-offs for different boundary conditions [3–6]. However, these approximations are inherently local. Each of them is valid only over a narrow vicinity of a specific thickness resonance. Consequently, there is a motivation for developing global long-wave formulations capable of capturing multiple high-frequency modes simultaneously. A recent progress in this direction was achieved for homogeneous coatings [7,8], where the multimode approximations are governed by differential equations with frequency-dependent coefficients.

B. Erbaş, J. Kaplunov: These authors contributed equally to this work

N. Ege (✉) · B. Erbaş
Department of Mathematics, Eskişehir Technical University, Yunus Emre Campus, Eskişehir 26470, Turkey
E-mail: nsahin@eskisehir.edu.tr

B. Erbaş
E-mail: berbas@eskisehir.edu.tr; b.erbas@keele.ac.uk

J. Kaplunov
Department of Continuum Mechanics, RWTH Aachen University, Kackertstraße 9 52072, Aachen, Germany
E-mail: kaplunov@km.rwth-aachen.de; j.kaplunov@keele.ac.uk

B. Erbaş · J. Kaplunov
School of Computer Science and Mathematics, Keele University, Stoke-on-Trent ST5 5BG, Staffordshire, UK

Published online: 26 February 2026

Theoretical analysis of micromechanical material properties is crucial for a variety of advanced applications, including modeling of heterogeneous structures, e.g. see [9]. Among the latter, functionally graded (FGM) elastic coatings play an important role in modern engineering applications due to their ability to enhance durability, wear resistance, thermal protection, and overall structural performance. Numerous studies have addressed various aspects of their static and dynamic behaviours [5,10–24]. However, a long-wave model for FGM coatings has not yet been established. Such a model is only known for low-frequency vibrations of thin FGM plates and shells [25–27]. The present paper develops a multimode framework for the anti-plane motion of a FGM coating extending the asymptotic analysis in [7]. The functional grading is embedded into the developed asymptotic procedure, resulting in effective coefficients depending on the frequency parameter and the through-thickness variation of material properties. This procedure extends the long-wave high-frequency approach initially established for thin homogeneous plates and shells [3]. The derived one-dimensional equation governs a multimode long-wave approximation for which a characteristic wavelength is much greater than the coating thickness. It is valid over a broad frequency range and is robust for analyzing forced vibrations under anti-plane shear loading prescribed along the upper face. At the same time, as might be expected, the above mentioned equation does not capture short-wavelength behaviour.

The studied 2D anti-plane time-harmonic problem is formulated in Section 2. The next section is concerned with multimode long-wave asymptotic analysis. Sections 4–6, consider special scenarios of transversely inhomogeneous coatings. In particular, Section 4 deals with a homogeneous case which readily follows from the general formulation. Coincidence with the previous results, see [7], is demonstrated. In Section 5, a two-layered coating is considered. The asymptotic predictions are tested by comparison with the exact solution presented in the Appendix. The FGM coating with material parameters varying across the thickness according to a power-law widely used in literature, e.g. see [28–30], is analyzed. Numerical results are presented for a specific value of the power exponent.

## 2 Problem formulation

Consider an elastic coating of thickness $H$ occupying the region $-\infty < x_1, x_3 < \infty$ and $0 \le x_2 \le H$ in the Cartesian coordinate system, see Figure 1. The problem variable parameters specifying mechanical properties of the plate are assumed to depend on the thickness variable. In particular, for the shear modulus $\mu = \mu(x_2)$, for density $\rho = \rho(x_2)$. For the anti-plane shear motion, the only non-zero displacement component $u(x_1, x_2)$ is orthogonal to the $x_1x_2$ plane. In this case, 2D antiplane motion for the coating can be written as

$$\sigma_{31,x_1} + \sigma_{32,x_2} + \rho(x_2)\omega^2 u = 0, \tag{1}$$

while the constitutive relations are given by

$$\sigma_{31} = \mu(x_2)u_{,x_1}, \quad \sigma_{32} \quad = \mu(x_2)u_{,x_2}. \tag{2}$$

In the above, $\sigma_{3i}$, $i = 1, 2$ denote stresses, and $\omega$ is circular frequency.

The layer is assumed to be fixed along its lower face and subject to a shear load $P(x_1)$ along its upper one, see Figure 1. We, therefore, impose the boundary conditions

$$\begin{aligned} u &= 0, \qquad && x_2 = 0, \\ \sigma_{32} &= P, \qquad && x_2 = H. \end{aligned} \tag{3}$$

We suppose that the thickness $H$ is small in comparison to a typical wavelength $L$, i.e.,

$$\eta = \frac{H}{L} \ll 1 \tag{4}$$

and in addition, without loss of generality, we restrict ourselves to a multimode frequency range where

$$\Omega = \frac{\omega H}{c_{20}} \sim 1 \tag{5}$$

with $c_{20}^2 = \mu_0/\rho_0$ with $\mu_0 = \mu(0)$ and $\rho_0 = \rho(0)$.

In the next section, we reduce the original 2D problem (1)–(3) to a 1D equation governing long-wave motion over the range (5) complementing earlier the asymptotic methodology for thin FGM plates and shells, [8,26] by the multimode procedure presented in [7,8].

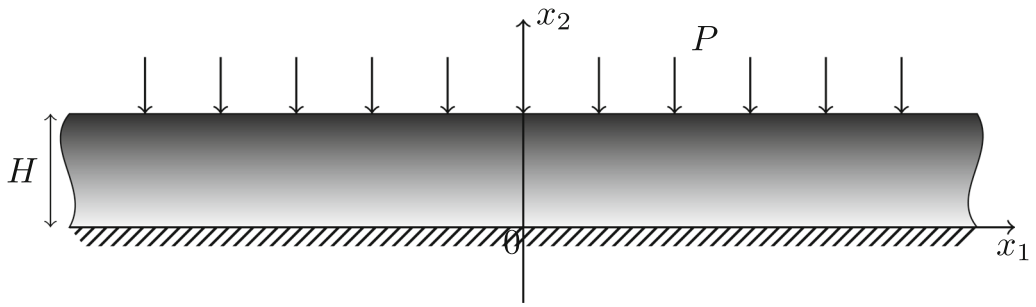



**Fig. 1** An elastic FGM thin coating

## 3 Multimode asymptotic approach

Let us scale the original variables according to the setting in the previous section. Consequently,

$$x_1 = L\xi, \qquad x_2 = H\zeta. \tag{6}$$

In addition, scale displacement and stress components as

$$u = Hu^*, \qquad \sigma_{31} = \eta\mu_0\sigma_{31}^*, \qquad \sigma_{32} = \mu_0\sigma_{32}^* \tag{7}$$

and

$$P = \mu_0 P_*. \tag{8}$$

We also set

$$\mu = \mu_0\mu_*(\zeta), \qquad \rho = \rho_0\rho_*(\zeta). \tag{9}$$

where $\mu_0$ and $\rho_0$ are constants defined above. All starred quantities in the relations above are assumed of the same asymptotic order.

Inserting the scalings given by formulae (7) into the equations of motion (1) and constitutive relations (2) and adopting non-dimensionless variables (6), we obtain

$$\eta^2\sigma_{31,\xi}^* + \sigma_{32,\zeta}^* + \rho_*\Omega^2 u^* = 0 \tag{10}$$

and

$$\sigma_{31}^* = \mu_* u_{,\xi}^*, \qquad \sigma_{32}^* = \mu_* u_{,\zeta}^*. \tag{11}$$

The boundary conditions become

$$\begin{aligned} u^* &= 0, \qquad \zeta = 0, \\ \sigma_{32}^* &= P_*, \qquad \zeta = 1. \end{aligned} \tag{12}$$

In what follows, we also use equations (10) and (11) written through the displacement. They become

$$\frac{\partial}{\partial\zeta}\left(\mu_*\frac{\partial u^*}{\partial\zeta}\right) + \eta^2\mu_*\frac{\partial^2 u^*}{\partial\xi^2} + \rho_*\Omega^2 u^* = 0. \tag{13}$$

We expand all starred quantities in an asymptotic series in powers of the small parameter $\eta$ as

$$f^* = f^{(0)} + \eta^2 f^{(1)} + \ldots, \tag{14}$$

where $f^* = \sigma_{3i}^*$ or $f^* = u^*$.

At leading order, we have from (13)

$$\frac{\partial}{\partial\zeta}\left(\mu_*\frac{\partial u^{(0)}}{\partial\zeta}\right) + \rho_*\Omega^2 u^{(0)} = 0 \tag{15}$$

with the boundary condition along the lower face $\zeta = 0$

$$u^{(m)} = 0 \tag{16}$$

with $m = 0$ at the moment.

Equation (15) has two linearly independent solutions. Denote the one satisfying the homogeneous boundary condition by $U^{(0)}(0) = 0$ and let $V^{(0)}(0) \neq 0$ be the second one nonzero at the lower boundary. Thus, the solution of the homogeneous equation (15), satisfying (16), takes the form

$$u^{(0)} = A_0(\xi)U^{(0)}(\zeta), \tag{17}$$

where $A_0(\xi)$ denotes an unknown 1D displacement amplitude.

At next order, we have from (13) an inhomogeneous equation given by

$$\frac{\partial}{\partial\zeta}\left(\mu_*\frac{\partial u^{(1)}}{\partial\zeta}\right) + \rho_*\Omega^2 u^{(1)} = -\mu_* U^{(0)}\frac{d^2A_0}{d\xi^2}. \tag{18}$$

The solution of this equation satisfying boundary condition (16) at $m = 1$ can be written as, see Appendix A for details,

$$u^{(1)} = A_1(\xi)U^{(0)}(\zeta) + \frac{d^2A_0}{d\xi^2}G(\zeta), \tag{19}$$

where $A_1(\xi)$ is an unknown function and

$$G(\zeta) = \frac{1}{W}\left(U^{(0)}(\zeta)\int_0^\zeta \mu_*(s)U^{(0)}(s)V^{(0)}(s)\,ds - V^{(0)}(\zeta)\int_0^\zeta \mu_*(s)\left(U^{(0)}(s)\right)^2 ds\right) \tag{20}$$

and, due to condition $U^{(0)} = 0$ at $\zeta = 0$, the Wronskian, $W$, can be written as

$$W = -U^{(0)'}V^{(0)}\big|_{\zeta=0}. \tag{21}$$

The combination of equations (17) and (19) gives

$$U^* = A(\xi)U^{(0)}(\zeta) + \eta^2\frac{d^2A(\xi)}{d\xi^2}G(\zeta), \tag{22}$$

where, now, $U^* = u^{(0)} + \eta^2 u^{(1)}$ and $A = A_0 + \eta^2 A_1$.

Finally, we apply boundary condition $(12)_2$ along the upper surface $\zeta = 1$ taking the form

$$\mu_*\frac{\partial U^*}{\partial\zeta} = P_*. \tag{23}$$

As a result, we arrive at the sought for 1D equation

$$\eta^2 T\frac{d^2A}{d\xi^2} + QA = \frac{P_*}{\mu_*(1)}, \tag{24}$$

where

$$Q = \left(U^{(0)}\right)'(1), \quad T = G'(1). \tag{25}$$

In the original variables (24) becomes

$$H^2T\frac{d^2A}{dx_1^2} + QA = \frac{P}{\mu(1)}, \tag{26}$$

whereas (22) takes the form

$$U = AHU^{(0)}(\zeta) + H^3\frac{d^2A}{dx_1^2}G(\zeta), \tag{27}$$

where $U = HU^*$. The coefficients $Q$ and $T$ in equation (26) depend upon the frequency parameter $\Omega$ leading to a multimode approximation.

Let us now present the two-term asymptotic solution of (24) setting

$$A = A_0 + \eta^2 A_1, \tag{28}$$

where

$$A_0 = \frac{P_*}{\mu_*(1)\, Q}, \quad A_1 = -\frac{T}{\mu_*(1)\, Q^2}\frac{d^2 P_*}{d\xi^2}. \tag{29}$$

The asymptotic expansion (28) fails near the thickness resonances, say, when $Q \sim \eta^2$. In the latter case, equation (24) governs a leading order approximation.

The obtained 1D equation is of the same for as that of a homogeneous coating to within the expressions for the effective coefficients which are frequency dependent as in homogeneous case. In the next section, we reduce the expressions for the aforementioned effective coefficients to the homogeneous counterparts earlier studied in [7].

## 4 A homogeneous coating

In the homogeneous setup, that is, for $\mu_* = \rho_* \equiv 1$, the linearly independent solutions of interest may be taken as

$$U^{(0)}(\zeta) = \sin \Omega\zeta, \qquad V^{(0)}(\zeta) = \cos \Omega\zeta. \tag{30}$$

It follows from (25), together with (20), that

$$G(\zeta) = \frac{\Omega\zeta \cos \Omega\zeta - \sin \Omega\zeta}{2\Omega^2}, \qquad Q = \Omega \cos \Omega, \qquad T = -\frac{\sin \Omega}{2}. \tag{31}$$

Substituting $U^{(0)}$ and $V^{(0)}$ in (22), we get

$$U^* = A(\xi) \sin \Omega\zeta + \eta^2 \frac{d^2 A(\xi)}{d\xi^2}\left(\frac{\Omega\zeta \cos \Omega\zeta - \sin \Omega\zeta}{2\Omega^2}\right). \tag{32}$$

The solution of the problem for a homogeneous coating was earlier obtained in [7] in the form

$$\eta^2 \hat{T}\frac{d^2 \hat{A}}{d\xi^2} + Q\hat{A} = P_* \tag{33}$$

and

$$\hat{U}^* = \hat{A}(\xi)U^{(0)}(\zeta) + \eta^2 \frac{d^2 \hat{A}(\xi)}{d\xi^2}\frac{\zeta \cos \Omega\zeta}{2\Omega}. \tag{34}$$

Here, $Q$ is given by (31), while

$$\hat{T} = \frac{\cos \Omega}{2\Omega} - \frac{\sin \Omega}{2}. \tag{35}$$

Let us now find the two-term asymptotic solution of (33) in the form

$$\hat{A} = \hat{A}_0 + \eta^2 \hat{A}_0 \tag{36}$$

having

$$\hat{A}_0 = \frac{P_*}{Q} = A_0, \quad \text{and} \quad \hat{A}_1 = -\frac{\hat{T}}{Q^2}\frac{d^2 P_*}{d\xi^2} = A_1 + \frac{\sin \Omega}{2Q^2}\frac{d^2 P_*}{d\xi^2}, \tag{37}$$

where $A_0$ and $A_1$ are given by (29). By substituting (36) in (34), we observe that, to within the error of $O(\eta^4)$, $U^* = \hat{U}^*$, as expected.

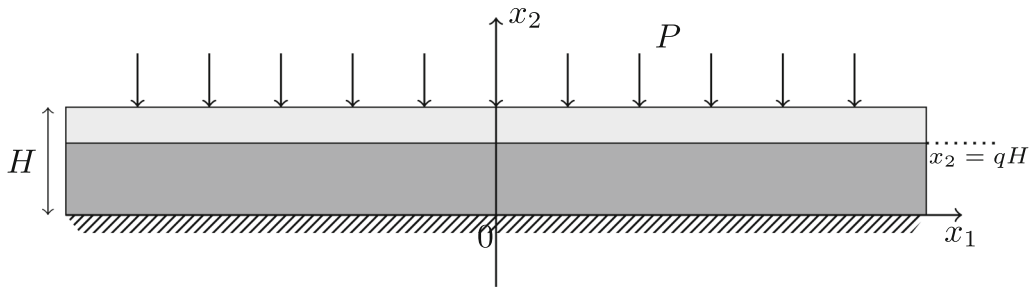



**Fig. 2** A two-layered inhomogeneous thin coating

## 5 A two-layered coating

As a next example consider a thin elastic coating composed of two layers each of which have different material parameters, see Figure 2. For the sake of simplicity, we assume a uniform shear modulus $\mu$ through the thickness and take the density to be piecewise defined, i.e.,

$$\rho(x_2) = \begin{cases} \rho_1, & qH \le x_2 \le \mathrm{H}, \\ \rho_2, & 0 \le x_2 \le q\ \mathrm{H}\,, \end{cases} \tag{38}$$

where $\rho_1$ and $\rho_2$ are constants and $0 \le q \le 1$.

The asymptotic solution readily follows from (22) for a 2-layered coating, since only the leading displacements $U^{(0)}$ and $V^{(0)}$ are needed. In this case, we sought for the solution of the problem (15) and (16) satisfying the continuity conditions

$$U^{(0)} = V^{(0)}, \qquad \left(U^{(0)}\right)' = \left(V^{(0)}\right)' \tag{39}$$

along the interface $\zeta = q$. We have

$$U^{(0)} = \begin{cases} U_1^{(0)}, & q \le \zeta \le 1, \\ U_2^{(0)}, & 0 \le \zeta \le q, \end{cases} \tag{40}$$

where

$$U_1^{(0)} = c_1 \sin(\gamma\Omega\zeta) + c_2 \cos(\gamma\Omega\zeta) \tag{41}$$

and

$$U_2^{(0)} = \sin(\Omega\zeta) \tag{42}$$

with

$$c_1 = \sin(\Omega q)\sin(\gamma\Omega q) + \frac{1}{\gamma}\cos(\Omega q)\cos(\gamma\Omega q), \tag{43}$$

$$c_2 = \sin(\Omega q)\cos(\gamma\Omega q) - \frac{1}{\gamma}\cos(\Omega q)\sin(\gamma\Omega q), \tag{44}$$

where $\gamma = \sqrt{\rho_1/\rho_2}$ and $\rho_n$, $n = 1, 2$ are mass densities in the corresponding layers.

Likewise, we may easily write $V^{(0)}$ as

$$V^{(0)} = \begin{cases} V_1^{(0)}, & q \le \zeta \le 1, \\ V_2^{(0)}, & 0 \le \zeta \le q, \end{cases} \tag{45}$$

for which

$$V_1^{(0)} = b_1 \sin(\gamma\Omega\zeta) + b_2 \cos(\gamma\Omega\zeta) \tag{46}$$

and

$$V_2^{(0)} = \cos(\Omega\zeta), \tag{47}$$

where

$$b_1 = \cos(\Omega q)\sin(\gamma\Omega q) - \frac{1}{\gamma}\sin(\Omega q)\cos(\gamma\Omega q), \tag{48}$$

$$b_2 = \cos(\Omega q)\cos(\gamma\Omega q) + \frac{1}{\gamma}\sin(\Omega q)\sin(\gamma\Omega q). \tag{49}$$

Then, we derive from (20) and $(25)_1$, respectively,

$$\begin{aligned} G(\zeta) =& \frac{\Omega\zeta\cos\Omega\zeta - \sin\Omega\zeta}{2\Omega^2}, \qquad 0 \le \zeta \le q, \\ G(\zeta) =& \frac{1}{4\gamma\Omega^2}\Big( (b_1\sin(\gamma\Omega\zeta) + b_2\cos(\gamma\Omega)\zeta)\left(-2\gamma\Omega\left(c_1^2 + c_2^2\right)(q-\zeta)\right. \\ & - 2c_1c_2\cos(2\gamma\Omega\zeta) + \left(c_1^2 - c_2^2\right)(\sin(2\gamma q\Omega) - \sin(2\gamma\Omega\zeta)) \\ & \left. + 2c_1c_2\cos(2\gamma q\Omega) + 2\gamma q\Omega - \gamma\sin(2q\Omega)\right) + 2\left(c_1\sin(\gamma\Omega\zeta) + c_2\cos(\gamma\Omega\zeta)\right) \\ & \Big( (b_1c_1 + b_2c_2)\gamma\Omega(q-\zeta) - \sin(\gamma\Omega(q-\zeta))((b_1c_1 - b_2c_2)\cos(\gamma\Omega(q+\zeta)) \\ & - (b_1c_2 + b_2c_1)\sin(\gamma\Omega(q+\zeta))) - \gamma\sin^2(q\Omega)\Big)\Big), \qquad q \le \zeta \le 1, \end{aligned} \tag{50}$$

and

$$Q = \Omega\left(\cos(\Omega q)\cos(\gamma(1-q)\Omega) - \gamma\sin(\Omega q)\sin(\gamma(1-q)\Omega)\right), \tag{51}$$

whereas $T$ is obtained by substituting (50) into $(25)_2$.

As an example, consider

$$P = P_0\cos\left(Kx_1/H\right), \tag{52}$$

where $K$ may be interpreted as $K = kH$ with $k$ being a wavenumber. In particular, we have for the interface $\zeta = q$

$$U = \frac{P_0\cos(Kx_1/H)}{\mu(1)(Q - K^2T)}\left(\sin\Omega q - \frac{K^2}{2\Omega^2}\left(\Omega q\cos\Omega q - \sin\Omega q\right)\right). \tag{53}$$

At leading order, we have from the latter

$$U = \frac{P_0\cos(Kx_1/H)}{\mu(1)(Q - K^2T)}\sin\Omega q. \tag{54}$$

In this case, the dispersion relation ($P = 0$) is given by

$$Q - K^2T = 0. \tag{55}$$

The leading order displacement $U^{(0)}$ and $V^{(0)}$ as well as coefficients $Q$ and $T$ are illustrated in Figures 3, 4a and 4b for several values of the frequency $\Omega$ obtained for the values of $K = 0.5$ and $\gamma = 1.75$. Figure 5 displays the dispersion curves corresponding to the exact solution (B13) and the refined asymptotic one (55) with the same values of $K$ and $\gamma$ as before. Although the asymptotic model is constructed for long-wave approximations valid over a narrow vicinity of cut-off frequencies similar to single-mode approximations investigated in a great detail, e.g., see [3] and references therein, it is clear that the asymptotic formulation accurately captures the exact dispersion curves in the $K \sim 1$ regime, particularly for higher frequencies.

Finally, we plot the comparison of the leading (eqn. (54)) and next order (eqn. (53)) approximate displacements along the interface $\zeta = q$ against the exact one (B15) at $x_1 = 0$. The excellent agreement between them are demonstrated in Figure 6 where, now, we take $q = 0.25$, $\gamma = 1.75$ with $K$ having the same value as above.

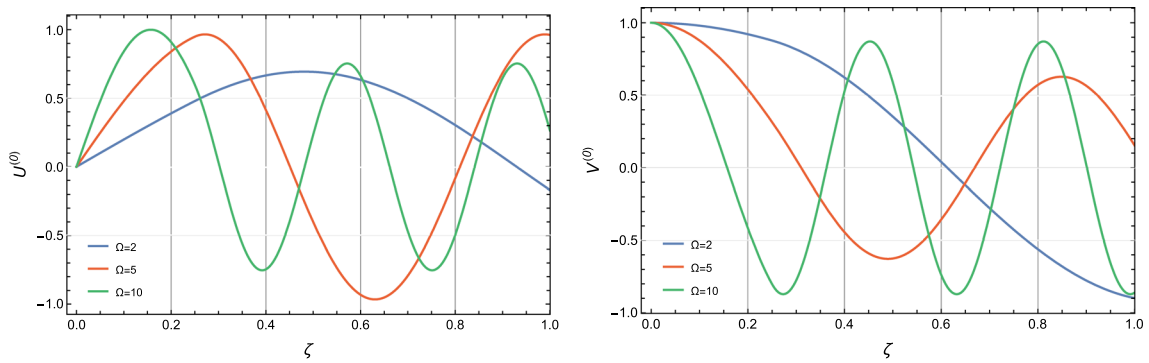



**Fig. 3** Eigenforms (a) $U^{(0)}$ and (b) $V^{(0)}$ of the 2-layered coating for several values of Ω for $q = 0.25$, $\gamma = 1.75$ and $K = 0.5$

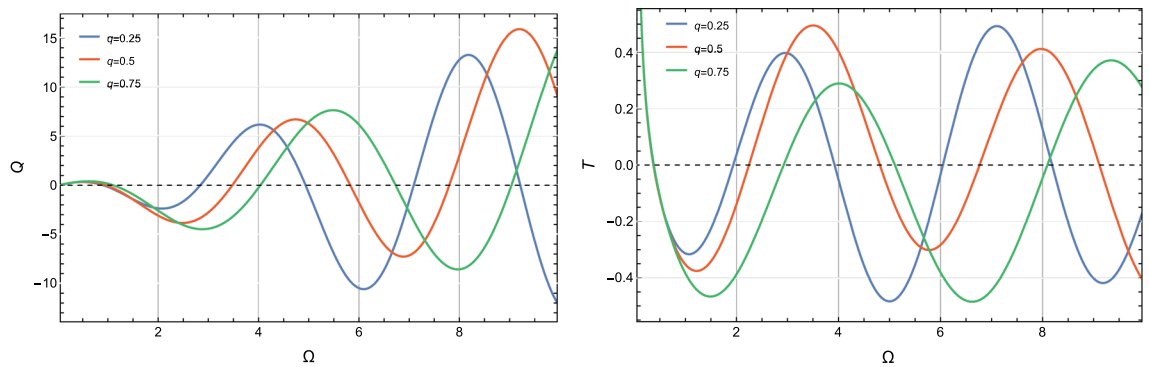



**Fig. 4** The variation of coefficients $Q$ and $T$ for $\gamma = 1.75$ and $K = 0.5$

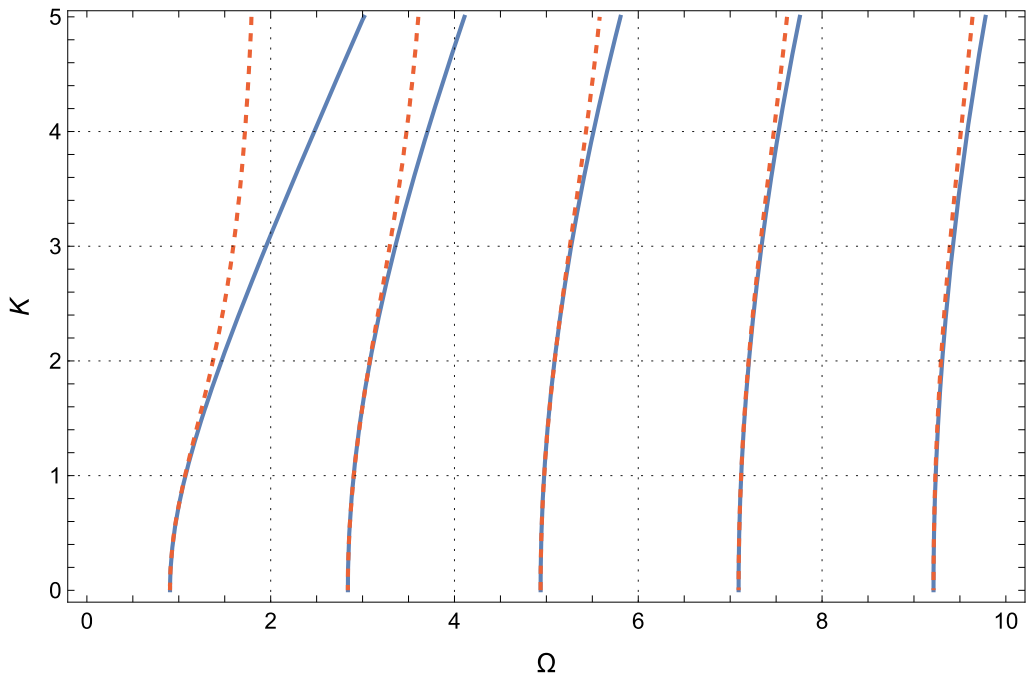



**Fig. 5** Comparison of the exact (blue) and asymptotic (red, dashed) dispersion curves corresponding to $q = 0.25$ and $\gamma = 1.75$

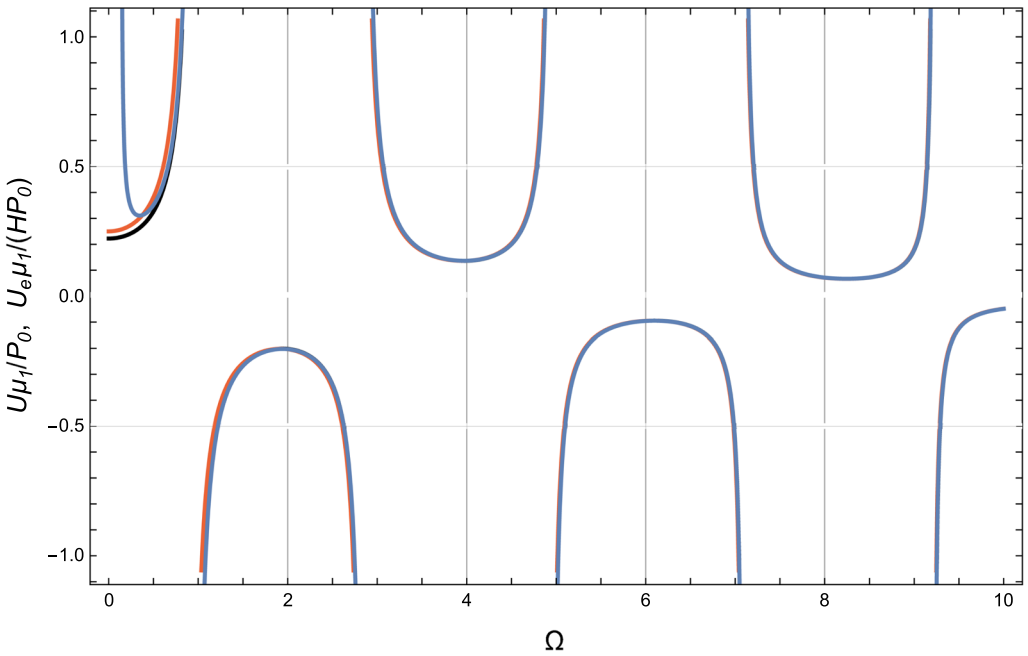



**Fig. 6** Comparison of the exact (black), leading (red) and refined (blue) asymptotic displacements along the interface, at $x_1 = 0$ for $q = 0.25$, $\gamma = 1.75$, $K = 0.5$ with $\mu_1 = \mu(1)$

## 6 FGM coating

Let us now consider a genuine functionally graded coating the material parameters of which obey a power-law rule adopted in numerous publications, e.g., see [28], also [29], that is,

$$\begin{aligned} \mu(\zeta) &= (\mu_1 - \mu_2)\zeta^p + \mu_2, \\ \rho(\zeta) &= (\rho_1 - \rho_2)\zeta^p + \rho_2 \end{aligned} \tag{56}$$

with the material properties of the plate varying from Nickel at the lower surface $\zeta = 0$ with $\mu_2 = 8.547 \times 10^{10}$ N/m$^2$, $\nu_2 = 0.31$ and $\rho_2 = 8900$ kg/m$^3$ to stainless steel at the upper surface $\zeta = 1$ with $\mu_1 = 7.579 \times 10^{10}$ N/m$^2$, $\nu_1 = 0.3262$ and $\rho_1 = 8166$ kg/m$^3$.

In this case, there is not much room for analytic expressions for the eigenfunctions $U^{(0)}$ and $V^{(0)}$ similar to (40) and (45) in the previous section, necessitating the numerical computation from the second order equation (15) where $\mu_* = \mu/\mu_0$, $\rho_* = \rho/\rho_0$ with $\mu_0 = \mu_2$, and $\rho_0 = \rho_2$. As before, $U^{(0)}$ satisfies the boundary condition (16), the second boundary condition imposed on $U^{(0)}$ as well as both boundary conditions on the function $V^{(0)}$ just need to guarantee their linear independence along with the requirement $V^{(0)}(0) \neq 0$. Eigenfunctions $U^{(0)}$ and $V^{(0)}$ are shown in Figures 7a and 7b at $p = 2$ for the frequencies $\Omega = 2$, 5 and 10.

Next, substituting the computed eigenfunctions $U^{(0)}$ and $V^{(0)}$ into formula (25), we have, after numerical integration, the sought for coefficients $Q$ and $T$ as functions of the frequency $\Omega$. They are shown in Figure 8 for the same values of the power $p$ as above.

Finally, using the evaluated coefficients in equation (25), we plot the dispersion curves, see Figure 9. In addition, we obtain the leading and next order approximations of the displacements along the upper face $\zeta = 1$. They are shown in Figure 10.

## 7 Conclusions

The main outcome of the present work is the derivation of a one-dimensional multimode long-wave equation governing the anti-plane motion of thin elastic coatings with thickness-dependent material properties, see (24). Starting from the two-dimensional time-harmonic problem for a layer clamped at its lower face and subjected to prescribed shear tractions on the upper face, a multimode asymptotic procedure is employed in the small

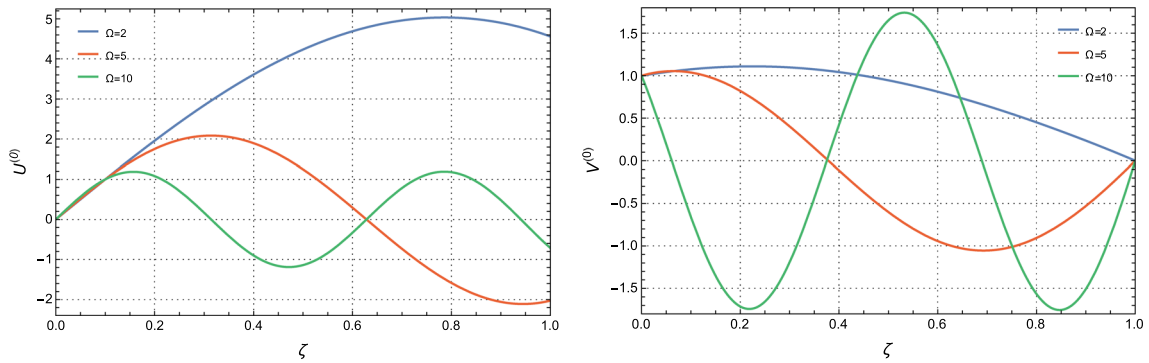



**Fig. 7** The variation of displacements (a) $U^{(0)}$ and (b) $V^{(0)}$ of the FGM coating for several values of Ω for the exponent $p = 2$

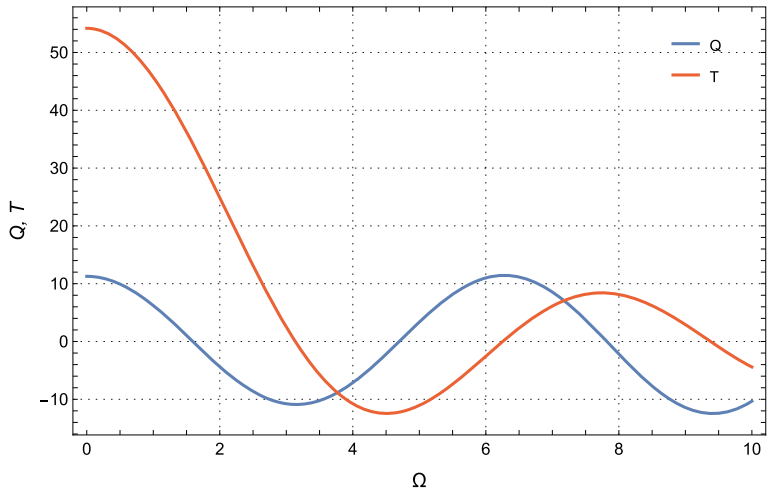



**Fig. 8** The variation of the coefficients $Q$ and $T$ with respect to Ω for the exponent $p = 2$

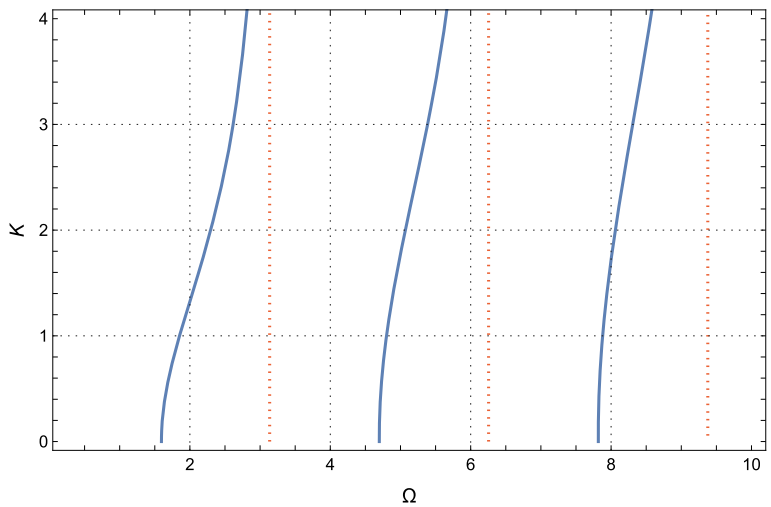



**Fig. 9** The dispersion curves (blue solid) for an elastic FGM coating calculated from the asymptotic relation (55) for the exponent $p = 2$. The vertical dashed lines correspond to $T = 0$

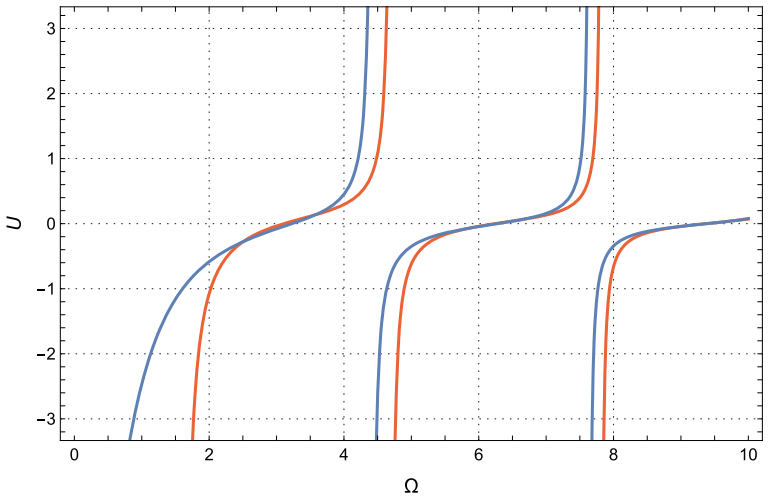



**Fig. 10** Leading (red) and refined (blue) asymptotic displacements for the FGM coating for the exponent $p = 2$ at $K = 0.5$

geometric thickness-to-wavelength ratio leading to the aforementioned effective amplitude equation together with the approximation of the displacement field across the thickness (22). The coefficients of this equation depend explicitly on the frequency parameter along with the shear modulus and density variations across the thickness, thereby enabling a unified description of all vibration modes in the long-wave regime.

The general formulation has been examined for several demonstrative scenarios. For a homogeneous coating, it simplifies to earlier reported closed-form expressions, and the resulting dispersion relation as well as displacement profiles agree with previously established results, see [7,8]. For a two-layered set-up, the asymptotic dispersion relation and interfacial displacements exhibit a full agreement with the exact solution derived from the original two-dimensional problem, including the vicinities of thickness resonances. For a genuinely functionally graded coating having power-law variations of shear modulus and density, numerically computed eigenfunctions enter the effective coefficients. The related dispersion curves and surface responses are demonstrated.

The dispersion phenomena analyzed in the paper corresponds to the long-wave behaviour of all vibration modes simultaneously. At the same time, the presented approximation breaks down over the short-wave regime. The obtained time-harmonic formulation, due to explicit dependence of the coefficients on the frequency parameter, can, in principle, be extended to transient problems via pseudo-differential operators in time. The developed framework is not restricted to the scalar anti-plane setting. The multimode asymptotic procedure can be adapted to three-dimensional problems extending the analysis presented in [8] dealing with homogeneous coatings (a work already in progress by the authors).

**Acknowledgements** The authors gratefully acknowledge the support from the Scientific and Technological Research Council of Türkiye (Tübitak), grant number 222N095.

**Open Access** This article is licensed under a Creative Commons Attribution 4.0 International License, which permits use, sharing, adaptation, distribution and reproduction in any medium or format, as long as you give appropriate credit to the original author(s) and the source, provide a link to the Creative Commons licence, and indicate if changes were made. The images or other third party material in this article are included in the article's Creative Commons licence, unless indicated otherwise in a credit line to the material. If material is not included in the article's Creative Commons licence and your intended use is not permitted by statutory regulation or exceeds the permitted use, you will need to obtain permission directly from the copyright holder. To view a copy of this licence, visit http://creativecommons.org/licenses/by/4.0/.

**Funding** Open access funding provided by the Scientific and Technological Research Council of Türkiye (TÜBİTAK).

**Declarations**

**Author Contribution** All author contributed equally to the manuscript.

**Data Availibility Statement** No datasets were generated or analysed during the current study.

**Competing interests** The authors declare no competing interests.

## Appendix A Particular solution

The particular solution $u_p^{(1)}$ of (18) may be obtained using the variation of parameters method. In terms of the two linearly independent solutions $U^{(0)}$ and $V^{(0)}$ of the associated homogeneous equation, it can be written as

$$u_p^{(1)} = D_1(\zeta)U^{(0)}(\zeta) + D_2(\zeta)V^{(0)}(\zeta), \tag{A1}$$

where $D_1$ and $D_2$ are the functions for which

$$D_1'U^{(0)} + D_2'V^{(0)} = 0. \tag{A2}$$

Now, we substitute (A1) into (18) having

$$D_1'\left(U^{(0)}\right)' + D_2'\left(V^{(0)}\right)' = -U^{(0)}A_{0,\xi\xi}. \tag{A3}$$

Using (A2) and (A3) and also taking into account (21), we obtain

$$D_1 = \frac{A_{0,\xi\xi}}{W}\int_0^\zeta \mu_* U^{(0)}V^{(0)}\,ds, \tag{A4}$$

$$D_2 = -\frac{A_{0,\xi\xi}}{W}\int_0^\zeta \mu_* (U^{(0)})^2\,ds. \tag{A5}$$

Then, the particular solution satisfying boundary condition (16) becomes

$$u_p^{(1)} = A_{0,\xi\xi}G(\zeta), \tag{A6}$$

where $G(\zeta)$ is given by (20).

## Appendix B Exact solution for a two-layered coating

Below, we present the exact solution for a two-layered coating considered in Section 5. The equation of motion, due to constant material parameters, is written as

$$\frac{\partial^2 u_n}{\partial x_1^2} + \frac{\partial^2 u_n}{\partial x_2^2} + \frac{\omega^2}{c_{2n}^2}u_n = 0, \qquad n = 1, 2, \tag{B7}$$

where $n = 1, 2$ corresponds to upper and lower layers, respectively and $c_{2n} = \sqrt{\mu/\rho_n}$ is the shear wave speeds in the respective layers.
Separating $\cos(Kx_1/H)$ and employing boundary condition (16), we promptly obtain from (B7) at $n = 2$

$$u_2 = C\sin(\alpha\zeta), \tag{B8}$$

where $\alpha^2 = \Omega^2 - K^2$ and $C$ is an arbitrary constant.
Next, we obtain the solution over the upper layer satisfying the continuity conditions (39) at the interface $\zeta = q$. It takes the form

$$u_1 = C_1\cos(\beta\zeta) + C_2\sin(\beta\zeta), \tag{B9}$$

where $\beta^2 = \gamma^2\Omega^2 - K^2$, $\gamma$ is defined as above, see Section 5, and

$$\begin{aligned} C_1 &= \sin(\alpha q)\,\cos(\beta q) - \frac{\alpha}{\beta}\cos(\alpha q)\sin(\beta q),\\ C_2 &= \sin(\alpha q)\,\sin(\beta q) + \frac{\alpha}{\beta}\cos(\alpha q)\cos(\beta q). \end{aligned} \tag{B10}$$

Now, using the dimensional counterpart of boundary condition (23), we get

$$F(K, \Omega) = \frac{P}{\beta\mu}, \tag{B11}$$

where

$$F(K,\Omega) = C_2 \cos\beta - C_1 \sin\beta \tag{B12}$$

with the equation

$$F(K,\Omega) = 0 \tag{B13}$$

implying the dispersion relation.
In addition, we have from the continuity conditions

$$C = \frac{PH}{\mu\beta\, F(K,\Omega)}. \tag{B14}$$

Finally, we have

$$u = \begin{cases} \dfrac{PH}{\mu\beta\, F(K,\Omega)}\, \sin(\alpha\zeta), & 0 \le \zeta \le q, \\ \dfrac{PH}{\mu\beta\, F(K,\Omega)} \Big(C_1 \cos(\beta\zeta) + C_2 \sin(\beta\zeta)\Big), & q \le \zeta \le 1. \end{cases} \tag{B15}$$

## References


1. Goldenveizer, A.: Theory of Thin Elastic Shells. Izdatel'stvo Nauka. Russian, Moscow (1976)
2. Aghalovan, L.A.: Asymptotic Theory of Anisotropic Plates and Shells. World Scientific, London (2015)
3. Kaplunov, J.D., Kossovich, L.Y., Kossovitch, L.Y., Nolde, E.: Dynamics of Thin Walled Elastic Bodies. Academic Press, New York (1998)
4. Kaplunov, J.: Long-wave vibrations of a thin walled body with fixed faces. The Quarterly J. Mech. Applied Math. **48**(3), 311–327 (1995)
5. Lashhab, M., Rogerson, G., Prikazchikova, L.: Small amplitude waves in a pre-stressed compressible elastic layer with one fixed and one free face. Z. Angew. Math. Phys. **66**(5), 2741–2757 (2015)
6. Pichugin, A.V., Rogerson, G.A.: An asymptotic membrane-like theory for long-wave motion in a pre-stressed elastic plate. Proc. R. Soc. Lond. A Math. Phys. Eng. Sci. **458**(2022), 1447–1468 (2002)
7. Erbaş, B., Itskov, M., Kaplunov, J., Prikazchikov, D.: Multimode long-wave approximation for a viscoelastic coating subject to antiplane shear. Z. Angew. Math. Phys. **75**(6), 234 (2024)
8. Ege, N., Erbaş, B., Kaplunov, J., Yücel, H.: Dynamics of a thin elastic coating. Int. J. Eng. Sci. **209**, 104221 (2025)
9. Kachanov, M., Sevostianov, I.: Micromechanics of Materials, with Applications, vol. 249. Springer, Berlin (2018)
10. Alexandrov, V., Mkhitaryan, S.: Contact Problems for Bodies with Thin Coatings and Interlayers. Nauka, Moscow (1983)
11. Benabdi, M., Roche, A.: Mechanical properties of thin and thick coatings applied to various substrates. Part i. an elastic analysis of residual stresses within coating materials. J. Adhes. Sci. Technol. **11**(2), 281–299 (1997)
12. Niklasson, A.J., Datta, S.K., Dunn, M.L.: On approximating guided waves in plates with thin anisotropic coatings by means of effective boundary conditions. J. Acoust. Soc. Am. **108**(3), 924–933 (2000)
13. Farrissey, L., McHugh, P.: Determination of elastic and plastic material properties using indentation: Development of method and application to a thin surface coating. Mater. Sci. Eng., A **399**(1–2), 254–266 (2005)
14. Zakharov, D., Nikonov, A.V.: Approximate description of the dynamics of thin isotropic elastic coatings and interlayers by using asymptotics of high order of accuracy. Mech. Compos. Mater. **41**(6), 527–534 (2005)
15. Rogerson, G.A., Sandiford, K.J., Prikazchikova, L.A.: Abnormal long wave dispersion phenomena in a slightly compressible elastic plate with non-classical boundary conditions. Int. J. Non-Linear Mech. **42**(2), 298–309 (2007)
16. Auriault, J.-L., Boutin, C.: Long wavelength inner-resonance cut-off frequencies in elastic composite materials. Int. J. Solids Struct. **49**(23–24), 3269–3281 (2012)
17. Zhang, Y., Sun, M.-J., Zhang, D.: Designing functionally graded materials with superior load-bearing properties. Acta Biomater. **8**(3), 1101–1108 (2012)
18. Bousser, E., Martinu, L., Klemberg-Sapieha, J.: Solid particle erosion mechanisms of protective coatings for aerospace applications. Surf. Coat. Technol. **257**, 165–181 (2014)
19. Vasiliev, A., Volkov, S., Aizikovich, S.: Approximated analytical solution of contact problem on indentation of elastic half-space with coating reinforced with inhomogeneous interlayer. Mater. Phys. Mech. **35**(1), 175–180 (2018)
20. Rogacheva, N.: Plates and beams of asymmetric structure in thickness. In: IOP Conference Series: Materials Science and Engineering, vol. 365, p. 042051 (2018). IOP Publishing
21. Gao, J., Zhang, M.-Q., Zhang, W.: Lamb waves propagation characteristics in functionally graded sandwich plates. Sensors **22**(11), 4052 (2022)
22. Ellahi, R.: Recent trends in coatings and thin film: Modeling and application. MDPI (2020)
23. Kim, J.-H., Lee, J.-H., Lee, S.-B., Kim, S.-J., Oh, M.-S.: Improved thermal satbility of al-Si alloy coated steel sheet with Cr thin film deposition. Archives of Metallurgy and Materials 69 (2024)
24. Erbaş, B., Itskov, M., Kaplunov, J., Rajagopal, K.R.: Response of a thin coating of a porous elastic material whose generalised young's modulus depends on the density. Math. Mech. Solids **30**(6), 1233–1248 (2025)
25. Kaplunov, J., Erbaş, B., Ege, N.: Asymptotic derivation of 2D dynamic equations of motion for transversely inhomogeneous elastic plates. Int. J. Eng. Sci. **178**, 103723 (2022)

26. Ege, N., Erbaş, B., Kaplunov, J., Noori, N.: Low-frequency vibrations of a thin-walled functionally graded cylinder (plane strain problem). Mech. Adv. Mater. Struct. **30**(6), 1172–1180 (2023)
27. Yücel, H.: Forced vibrations of a FGM thin-walled cylinder under fluid loading. Z. Angew. Math. Phys. **76**(1), 3 (2025)
28. Loy, C., Lam, K., Reddy, J.: Vibration of functionally graded cylindrical shells. Int. J. Mech. Sci. **41**(3), 309–324 (1999)
29. Iqbal, Z., Naeem, M.N., Sultana, N.: Vibration characteristics of FGM circular cylindrical shells using wave propagation approach. Acta Mech. **208**(3), 237–248 (2009)
30. Huang, G.-Y., Wang, Y.-S., Gross, D.: Fracture analysis of functionally graded coatings: antiplane deformation. Eur. J. Mech. A-Solid. **21**(3), 391–400 (2002)

**Publisher's Note** Springer Nature remains neutral with regard to jurisdictional claims in published maps and institutional affiliations.